Dalton Transactions

Dicopper(I) Complexes of a Binucleating, Dianionic, Naphthyridine Bis(amide) Ligand

Journal:	*Dalton Transactions*
Manuscript ID	DT-ART-01-2025-000034.R1
Article Type:	Paper
Date Submitted by the Author:	11-Feb-2025

Complete List of Authors:	Sévery, Laurent; University of California Berkeley, Department of Chemistry; Lawrence Berkeley National Laboratory, Chemical Sciences Division Wheeler, T. Alexander; University of California Berkeley, Department of Chemistry; Lawrence Berkeley National Laboratory, Chemical Sciences Division Nicolay, Amelie; University of California Berkeley, Department of Chemistry Teat, Simon; Lawrence Berkeley National Laboratory, Advanced Light Source Tilley, T.; University of California Berkeley, Department of Chemistry; Lawrence Berkeley National Laboratory, Chemical Sciences Division

Dicopper(I) Complexes of a Binucleating, Dianionic, Naphthyridine Bis(amide) Ligand

Authors: Laurent Sévery,[1,2] T. Alexander Wheeler,[1,2] Amelie Nicolay,[1] Simon J. Teat,[3] and T. Don Tilley[1,2]*

Affiliations:
[1]Department of Chemistry, University of California, Berkeley, Berkeley, CA 94720-1460, USA
[2]Chemical Sciences Division, Lawrence Berkeley National Laboratory, Berkeley, CA 94720, USA
[3]Advanced Light Source, Lawrence Berkeley National Laboratory, Berkeley, CA 94720, USA

Abstract

The dinucleating ligand, 1,8-naphthyridine-2,7-bis(2,6-diisopropylphenyl)carboxamide (**NBDA**), was synthesized by palladium-catalyzed aminocarbonylation. This ligand was treated with two equivalents of mesitylcopper(I) in the presence of [^{n}Bu$_4$N]X (X = Cl, N$_3$) to give the anionic complexes [^{n}Bu$_4$N][Cu$_2$(**NBDA**)(μ-Cl)] and [^{n}Bu$_4$N][Cu$_2$(NBDA)(μ-N$_3$)]. Treatment of H$_2$**NBDA** with mesitylcopper(I) and two equivalents of xylyl isocyanide led to the formation of a charge-neutral dicopper(I) complex, [Cu$_2$(**NBDA**)(CNXyl)$_2$], displaying two isocyanide ligands, each terminally bound to one of the copper atoms. The complexes were characterized by NMR and IR spectroscopy, as well as by single-crystal X-ray diffraction analysis. Electrochemical characterization of the complexes using cyclic voltammetry revealed a reversible ligand-based reduction between –1.65 and –2.0 V vs. Fc/Fc$^+$. DFT calculations suggest a more ionic bonding character and weaker Cu–Cu interactions in the **NBDA** complexes compared to those with other 1,8-naphthyridine-based ligands. This is congruent with intermetallic separations of over 3 Å induced by relatively strong coordination of the copper atoms to the amide nitrogen donor atoms observed in the solid state molecular structures.

Introduction

Bimetallic reaction centers play a prominent role in numerous chemical processes for biological and synthetic catalytic systems.[1–5] These catalytic sites rely on the interplay of the chemical and/or electronic properties of the two metal centers to perform distinct transformations, enabled by metal-metal cooperation.[6,7] Such cooperative effects have been difficult to deconvolute, and for this purpose a number of structural and functional model systems have been developed using appropriately designed coordination scaffolds. These models facilitate the investigation of the physical and chemical properties of multimetallic complexes and enzymatic active sites.[8–15]

In this context, 1,8-naphthyridine ligands have been used to study metal-metal interactions between transition metals for over 40 years.[16–20] This binucleating ligand scaffold can be equipped with additional coordinating functional groups at the 2 and 7 naphthyridine positions. These substituents or “side arms” provide a chelating binding environment or coordination pocket for each metal, while the rigid 1,8-naphthyridine backbone enforces a short intermetallic distance. The naphthyridine side arms dictate crucial electronic and geometric properties of the coordination pockets, such as the metal-metal separation distance.[21–23] In recent years, new 1,8-naphthyridine-based ligands have been developed for the study of dicopper complexes, in the context of relevance to biological and catalytic systems, and for applications in small molecule activation.[5,24–27]

The 1,8-naphthyridine-based ligands investigated for dicopper complexation are generally charge-neutral,[28–33] with donor side-arm groups such as pyridinyl, iminyl, and R$_2$PE- (E = CH$_2$, O) (Figure 1a). The copper ions in these complexes are typically in the +I oxidation state, but higher oxidation states

have also been described.[28] Dicopper(I) complexes of this type often possess two additional bridging ligands leading to pseudo-tetrahedrally coordinated copper atoms. A type of charge-neutral 1,8-naphthyridine-based ligand developed in this laboratory features dipyridyl side arms (Figure 1b).[25,34] Initially developed for dicobalt complexes, these ligands (DPEN for R = CH_3; DPFN for R = F) have been used to study dicopper complexes in the +I to +III oxidation states, with a variety of bridging ligands.[35–39]

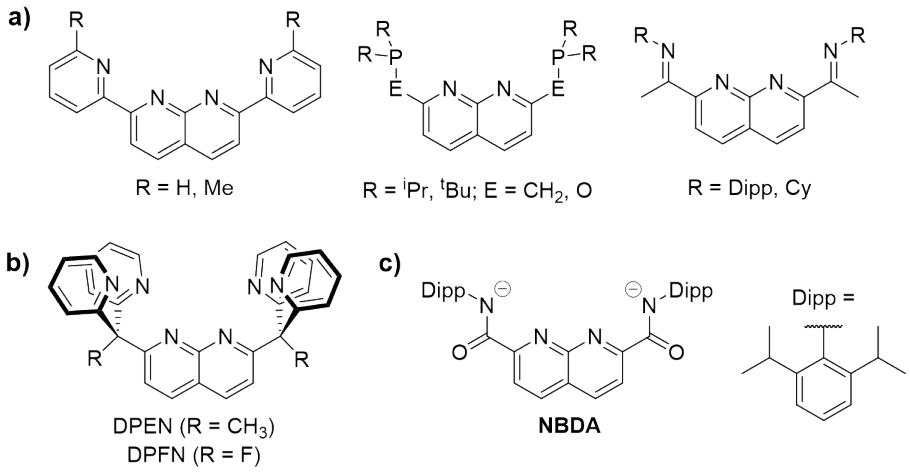

Figure 1. Different dinucleating ligands based on the 1,8-naphthyridine scaffold symmetrically substituted at the 2 and 7 positions. a) charge-neutral bidentate designs. b) charge-neutral tridentate designs. c) dianionic bidentate) design.

Most contemporary 1,8-naphthyridine ligands feature charge-neutral functional side arms, while charged ligand designs are less widely explored, despite the prevalence of negatively charged ligands in multimetallic active sites encountered in biological systems.[40,41] Furthermore, monometallic copper complexes with anionic ligands based on a pyridine scaffold have been extensively explored for their oxygen activation and C–H bond activation, for example by Tolman and coworkers.[42–44] Anionic naphthyridine-based ligands therefore represent interesting targets for study, as they are expected to impart unique electronic and chemical properties to the metals. Notably, a simple example of such a ligand, 1,8-naphthyridine-2,7-dicarboxylate, has been employed for coordination of second-row transition metals.[19,45] However, anionic 1,8-naphthyridine-based ligands with other side arms have not been broadly established in bimetallic chemistry.

A rare example of a dianionic 1,8-napthyridine ligand with amido-substituents at the 2 and 7 positions (Figure 1c) was reported by Gagnon and Tolman.[46] The synthetic method involving a bis(formyl) intermediate provided a low yield, but was used to obtain a dicopper(I) complex with a single bridging chloride ligand. These results motivated the search for a scalable synthesis of the 1,8-naphthyridine bis-amide ligand, to thoroughly investigate the effect of the ligand's negative charge on the structures and reactivity of coordinated dicopper units.

This contribution describes a convenient one-step synthesis of the dianionic ligand, 1,8-naphthyridine-2,7-bis(2,6-diisopropylphenyl)carboxamide (**NBDA**; Figure 1c) from the readily available 2,7-dichloro-1,8-naphthyridine precursor. This new preparative route enables detailed studies of its coordination chemistry. The new dicopper complexes obtained with this scaffold exhibit distinct structural properties that reflect the anionic nature of the amido side arms. Such insights were obtained through solid-state structural analyses, electrochemical studies and DFT calculations.

Results and Discussion

Synthesis of H_2**NBDA** from commercially available 2,7-dichloro-1,8-naphthyridine was achieved by palladium-catalyzed aminocarbonylation using 2,6-diisopropylphenylamine under a CO atmosphere (5 atm), with the procedure adapted from El-ghayoury. (Scheme 1).[47] Purification by silica gel column chromatography followed by recrystallization from isopropanol gave H_2**NBDA** in 56% isolated yield. Characteristic amide N-H stretching vibrations at 3352 cm^{-1} and 3296 cm^{-1} were observed in the IR spectrum of H_2**1** (Figure S1), and the ^{1}H NMR spectrum of H_2**NBDA** matches the one previously reported.[46]

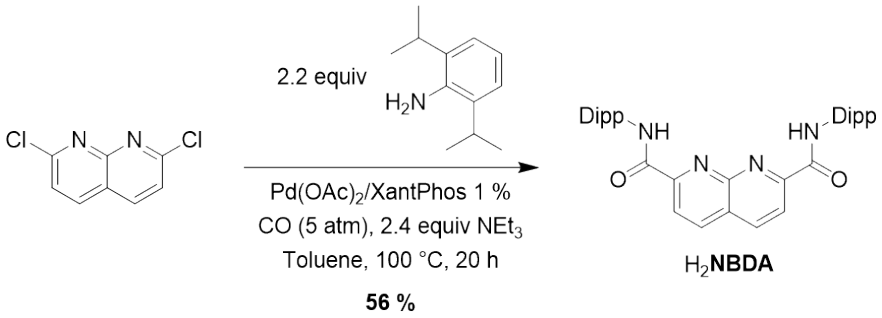

*Scheme 1. Synthesis of the H_2**NBDA** ligand. Dipp is 2,6-diisopropylphenyl.*

With bis-amide H_2**NBDA** in hand, the metallation with copper was investigated. The initial synthesis of the bridging chloride complex [^{n}Bu$_4$N][Cu$_2$(**NBDA**)(μ-Cl)] (**1**) followed the two-step procedure reported by Gagnon.[46] However, double deprotonation of the ligand in situ followed by addition of 2.0 equiv of CuCl and 1.0 equiv of tetrabutylammonium chloride ([^{n}Bu$_4$N]Cl) resulted only in the formation of a small amount of product. The synthesis of **1** in significantly higher yield was achieved by employing mesitylcopper(I) (CuMes) as the copper source and base. Thus, reaction of H_2**NBDA** with 2.05 equiv of CuMes in THF, in the presence of 1.0 equiv of [^{n}Bu$_4$N]Cl (Scheme 2), led to the formation of **1**. The complex was purified by filtration through celite and subsequent crystallization to give a yield of 86 %. In the absence of [^{n}Bu$_4$N]Cl, the reaction between CuMes and H_2**NBDA** was sluggish at 22 °C and after 24 h gave a red-brown solution, and ^{1}H NMR spectroscopy indicated the presence of both mesitylene and H_2**NBDA**.

The ^{1}H NMR spectrum of **1** in dichloromethane-d_2 is in good agreement with that previously reported (with DMSO-d_6 solvent).[46] A red shift of the carbonyl stretching band observed in **1** (1603 cm^{-1}) relative to that of the free ligand (1680 cm^{-1}) reflects the increased electron density on the amide after deprotonation (Figure S2).

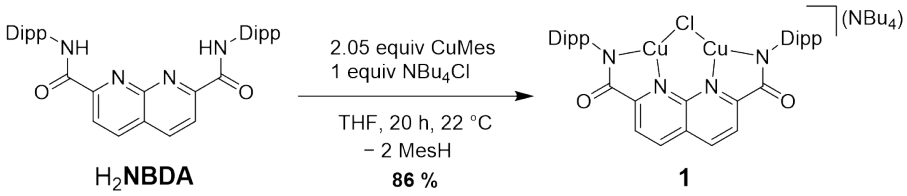

*Scheme 2. Synthesis of complex **1**.*

The solid-state molecular structure (Figure 2), as determined by single-crystal X-ray diffraction, is consistent with the ^{1}H NMR spectrum. The Cu–Cu distance in **1** is 2.98(3) Å, which is longer than for other naphthyridine dicopper(I) complexes bridged by a chloride anion.[30,32,36,48] The Cu–N_{Amide} distance of 1.956(4) Å is substantially shorter than the Cu–N_{Naph} distance of 2.12(2) Å, leading to a distorted trigonal coordination for each metal, with an average angle ∠(N_{Naph}-Cu-N_{Amide}) of 81.3(2)°. The {(N_{Naph})$_2$-(N_{Amide})$_2$-Cu$_2$-Cl} moiety forms a near-planar core, with a slight twisting of the naphthyridine and the carbonyl groups from the carboxamide side-arms.

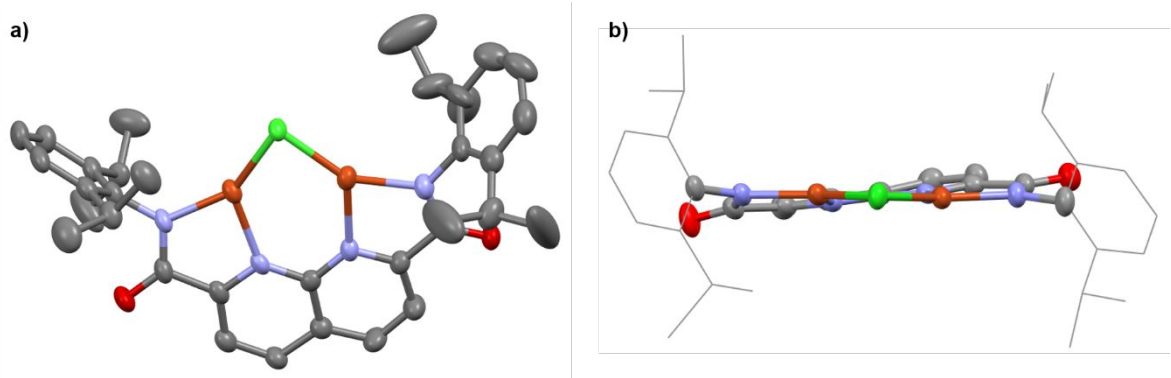

*Figure 2. Solid-state molecular structure of complex **1** (50 % probability ellipsoids) viewed from a) the side and b) the top. One additional molecule of **1** in the asymmetric unit as well as counterions, solvent molecules and hydrogen atoms are omitted for clarity. Carbon atoms are displayed in grey, oxygen atoms are displayed in red, nitrogen atoms in blue, chlorine atoms in green and copper atoms in orange. In b) the side-arms are displayed as wireframe for better clarity.*

To gain a better understanding of the electronic properties of the dicopper complexes supported by the **NBDA** ligand, the synthesis of a bridging azide complex was targeted. Similar to CO, the azide ligand (N_3^-) has been used as a IR spectroscopic handle to study the degree of metal-ligand interaction and electronic properties of metal complexes.[49–51] The azide complexes of DPFN (bis(dipyridylfluoromethyl)-1,8-naphthyridine) and **NBDA** were envisioned as comparative models to evaluate the effect of formal negative charges onto the naphthyridine ligand backbone.

The reaction of one equiv of $[^nBu_4N]N_3$ with the previously reported dicopper complex $[Cu_2(DPFN)(\mu\text{-MeCN})][NTf_2]_2$ (NTf_2 is bis(trifluoromethanesulfonyl)imidate),[35] containing a bridging acetonitrile ligand, resulted in formation of the N_3-bridged, monocationic dicopper complex $[Cu_2(DPFN)(\mu\text{-}N_3)][NTf_2]$ (**2**) in 81 % yield (Scheme 3a). The anionic, N_3-bridged complex $[^nBu_4N][Cu_2(NBDA)(\mu\text{-}N_3)]$ (**3**), was obtained through an analogous procedure involving metallation of H_2**NBDA** with 2.05 equiv of CuMes followed by addition of 1.0 equiv of $[^nBu_4N]N_3$ (Scheme 3b), in a yield of 72%. Crystals of the two complexes suitable for single-crystal X-ray diffraction were grown by vapor diffusion of diethyl ether into saturated THF solutions.

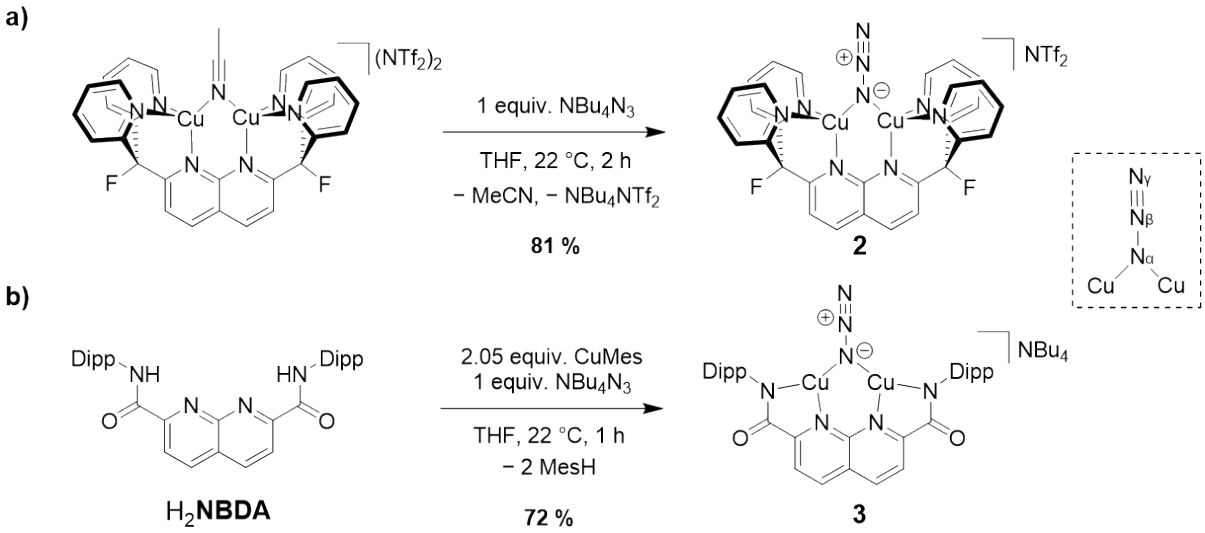

*Scheme 3. a) Synthesis of complex **2**. b) Synthesis of complex **3**.*

The solid-state molecular structures of **2** and **3** reveal a symmetrical coordination of the azide ligand in a bridging position between the two copper atoms (Figure 3). For complex **2**, the Cu–Cu distance is 2.609(1) Å while the $Cu–N_{Azide}$ distances are 1.941(1) Å and the average Cu–N distance involving the

DPFN ligand is 2.07(1) Å. The azide ligand lies in the plane of the naphthyridine fragment, and a Cu-N_{Azide}-Cu bond angle of 84° is observed. The unit cell of complex **3** contains two dicopper complexes featuring a longer average (of the two molecules in the asymmetric unit) Cu–Cu distance of 3.08(1)Å, and the bridging azide ligand is tilted out of the plane defined by the naphthyridine ligand by 30°. The NMR spectrum of **3** at ambient temperature suggests C_{2v} symmetry for **3**, and it is presumed that solid-state packing effects are responsible for the deviation from planarity. The Cu–N_α bond distances average to 1.88(1) Å, which is slightly shorter than in the DPFN complex. The average Cu–N_{Naph} (2.18(1) Å) and Cu–N_{Amide} (1.92(1) Å) distances are comparable to the corresponding distances in **1**, whereas the naphthyridine core in **3** is fully planar. The average angle ∠(N_{Naph}-Cu-N_{Amide}) is 80.8(3)°, with a distorted trigonal copper coordination geometry very similar to that in complex **1**.

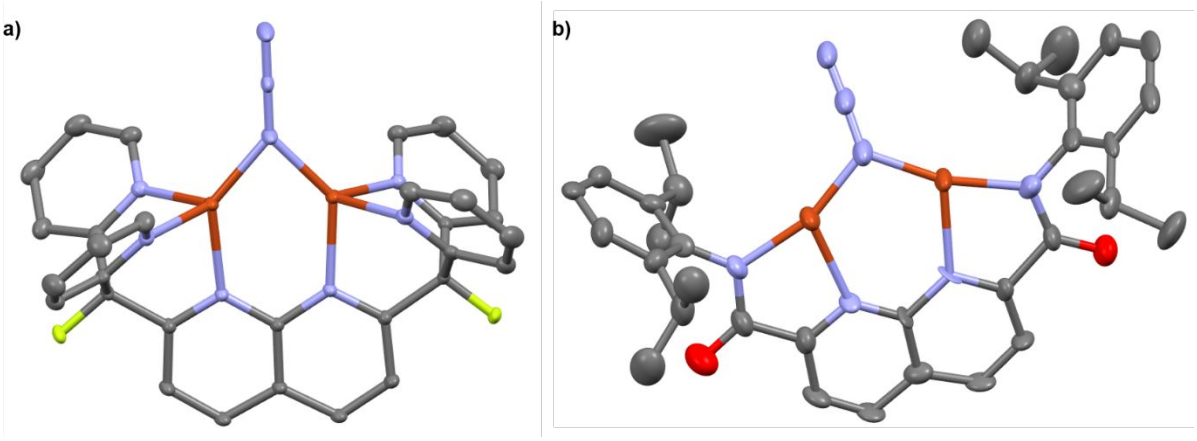

*Figure 3. a) Solid-state molecular structure of complex **2** (50 % probability ellipsoids). b) Solid-state molecular structure of complex **3** (50 % probability ellipsoids). One additional molecule of **3** in the asymmetric unit as well as counterions, solvent molecules and hydrogen atoms in both structures are omitted for clarity.*

The azide ligands in **2** and **3** exhibit similar metrical parameters in the solid state. The N–N bond distances associated with the donor nitrogen atom, $d(N_\alpha – N_\beta)$, are 1.179(1) Å (for **2**) and 1.21(4) Å (for **3**), while $d(N_\beta–N_\gamma)$ are 1.152(1) Å (for **2**) and 1.16(2) Å (for **3**). These distances are similar to those observed for the free azide anion.[52] The IR spectra of these complexes also reflect weak activation of the azide, with bands at 2079 cm^{-1} (**2**) and 2070 cm^{-1} (**3**) (Figures S3 and S4) attributed to the azide asymmetrical stretching mode (the free azide stretching mode is at 1986 cm^{-1} in the gas phase and 2048 cm^{-1} in aqueous solution).[53] As in the chloride-bridged bis-amide complex, the metal centers in **3** adopt a distorted trigonal coordination geometry. The distorted tetrahedral geometry for both copper atoms in **2** is consistent with other complexes containing the DPFN ligand.

Despite the different coordination environments for the copper atoms in **2** and **3**, the azide ligands in these complexes appear to have similar electronic charateristics. This would suggest that the binding of the azide by dicopper(I) has a large ionic contribution. To further examine the effects of the dianionic nature of the **NBDA** ligand on structure, it was of interest to compare the properties of complexes with a neutral bridging ligand. For this purpose, xylyl isocyanide (CNXyl), a strong σ-donor, was chosen as it is expected to both solubilize and stabilize a neutral dicopper(I) species with the **NBDA** scaffold. Furthermore, the previously reported dicationic complex $[Cu_2(DPEN)(\mu\text{-CNXyl})](PF_6)_2$ provides a good basis for comparisons.[34]

The reaction of H_2**NBDA** with 2.05 equivs of CuMes in the presence of 1.0 equiv of CNXyl in THF led to the formation of an orange solution, which after filtration and layering with pentane produced a small amount of an orange-red crystalline solid. A ^{1}H-NMR spectrum of this material indicates the presence of coordinated **NBDA** and coordinated isocyanide in a 1:2 ratio, suggesting the formation of a

bimetallic complex with two CNXyl ligands. Repetition of the reaction with 2.0 equivs of CNXyl produced the same product, identified as the charge-neutral dicopper(I) complex [Cu(**NBDA**)$(CNXyl)_2$] (**4**) in excellent yield (92%, Figure 4).

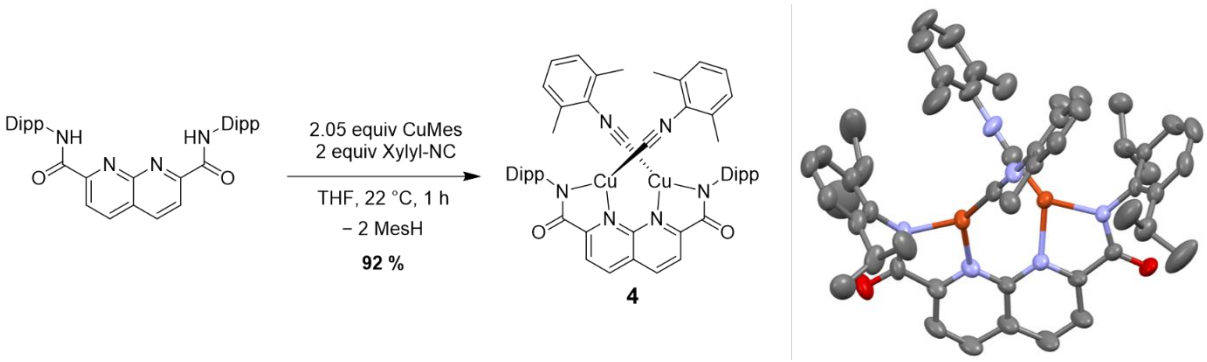

*Figure 4. Synthesis and crystal structure of complex **4** (50 % probability ellipsoids). Additional molecules of **4** in the asymmetric unit as well as solvent molecules and hydrogen atoms are omitted for clarity.*

X-ray diffraction quality crystals of **4** were obtained by vapor diffusion of diethyl ether into a benzene solution of the complex. In contrast to a related DPEN complex, in which the isocyanide ligand takes up a bridging position between two copper atoms, complex **4** contains two terminally bound xylyl isocyanide ligands, each coordinating to one of the copper centers. The copper atoms protrude from the plane defined by the naphthyridine by 0.6 Å, likely due to the steric requirements of the xylyl substituents. Complex **4** possesses a C_2 rotational axis that extends through the central C–C bond of the naphthyridine, resulting in axial chirality for the complex. The unit cell contains two molecules of **4** with counterrotating C_2 axes, leading to an overall achiral solid-state structure.

The average Cu–Cu distance is 3.04(2) Å, which is similar to those observed in complexes **1** and **3** and significantly longer than that in the related DPEN complex (Cu–Cu distance of 2.36 Å with one bridging xylyl isocyanide).[34] The average Cu–N_{Naph} bond distance in **4** (2.04(1) Å) is shorter than in the anionic complexes **1** and **3**, while the average Cu–N_{Amide} distance (1.97(1) Å) is approximately the same. The average angle ∠(N_{Naph}-Cu-N_{Amide}) is 81.3(2)° indicated a similar copper coordination geometry as in the anionic complexes. The average C≡N bond length of the terminally coordinated isocyanide ligands in **4** is 1.17(1) Å, corresponding to a minimal elongation compared to free xylyl isocyanide.[54] The average Cu–C bond distances (1.83(1) Å) are among the shortest reported for copper isocyanide complexes.[55] A very intense IR band at 2145 cm^{-1} attributed to the isocyanide C–N stretching mode was observed for **4**, representing a blue-shift relative to that of the free ligand (2119 cm^{-1}) (Figure S5). These observations suggest that the isocyanide acts as a strong σ-donor but experiences only weak π-back-bonding from the copper atoms.[56] The near-linear isocyanide moiety (C_{Xylyl}–N–C angle of 177(3)°) supports this assessment.

DFT calculations were used to further elucidate the bonding interactions in **1**-**4**, as well as the previously reported complexes $[Cu_2(DPFN)(\mu\text{-}Cl)]^+$ and $[Cu_2(bpnp)(\mu\text{-}Cl)_2]$ (bpnp is 2,7-dipyridiyl-1,8-naphthyridine).[36,48] The geometries of all complexes were optimized in vacuum using the corresponding crystal structures as starting points, omitting counterions and any solvent molecules. Optimization of the geometries was performed using the def2-SVP basis set with the ωB97X-D functional,[57] then further optimized in the def2-TZVP basis set. Natural bond orbital (NBO) analysis was performed on all complexes to determine the main orbital contributions to the ligand-metal interactions.

Wiberg bond orders for bonds between copper and its donor atoms are given in Table 1. The intermetallic interaction between the Cu(I) atoms in the **NBDA** complexes appears to be weaker than those in the other naphthyridine-based complexes, independent of the nature of the ligand side arms. The Cu–N_{Naph} bond orders are slightly lower for **1** and **3**, relative to their DPFN counterparts. The Cu–N_{Amide} bond orders in the **NBDA** complexes are slightly higher than those of the Cu–N_{Pyr} bonds in the DPFN and bpnp complexes, suggesting an additional ionic bonding contribution in complexes with the formally dianionic ligand backbone. This is also reflected in the natural charges of copper in **1** (+0.52) and **3** (+0.60), which are somewhat more positive when compared to complexes with the DPFN ligand and the same bridging ligand (+0.45 for $[Cu_2(DPFN)(\mu\text{-}Cl)]^+$ and +0.53 for complex **2**; see Table S1 in SI).

Table 1. Wiberg bond orders for the bonds involving copper and total Wiberg bond orders in the selected complexes.

	Cu–Cu	**Cu–X (bridging ligand)**	**Cu–N_{Naph}**	**Cu–L (sidearm)**	**Cu (total)**	**L (sidearm total)**
$[Cu_2(\mathbf{NBDA})(\mu\text{-}Cl)]^-$ (**1**)	0.04	0.44	0.14	0.29	1.03	3.07
$[Cu_2(DPFN)(\mu\text{-}N_3)]^+$ (**2**)	0.09	0.33	0.21	0.23	1.31	3.23
$[Cu_2(\mathbf{NBDA})(\mu\text{-}N_3)]^-$ (**3**)	0.03	0.32	0.13	0.30	0.97	3.08
$[Cu_2(\mathbf{NBDA})(CNXyl)_2]$ (**4**)	0.04	0.66	0.23	0.32	1.53	3.09
$[Cu_2(DPFN)(\mu\text{-}Cl)]^+$	0.13	0.44	0.20	0.21	1.37	3.23
$[Cu_2(bpnp)(\mu\text{-}Cl)_2]$	0.07	0.36	0.16	0.25	1.35	3.24

The total Wiberg bond index, corresponding to the sum of all bond indices for a given atom, was evaluated for the copper and the side arm nitrogen (donor) atoms. Within the complexes containing a bridging chloride, the copper atoms in **1** display a lower total Wiberg bond index (1.03) than in $[Cu_2(DPFN)(\mu\text{-}Cl)]^+$ (1.37) or $[Cu_2(bpnp)(\mu\text{-}Cl)_2]$ (1.35), indicating a lower coordinative saturation of Cu in **1**. A similar difference in bond order is observed between azide-bridged complexes **3** (0.97) and its DPFN analogue **2** (1.31).

For the overall neutral complex **4**, a stronger interaction of copper with the naphthyridine nitrogen (Cu–N_{Naph} bond order of 0.23) is observed, along with a lower overall charge on the **NBDA** ligand relative to the anionic complexes **1** and **3** (–1.32 versus –1.53 for **1** and -1.54 for **3**). This could be interpreted as a transfer of electronic density into the isocyanide ligands. NBO analysis of **4** suggests that some back-bonding from Cu 3d orbitals into the C–N π^* orbitals is present. Stabilization of Cu(I) by the isocyanide as well as the slight increase of interactions with the naphthyridine is reflected in the largest total Wiberg bond order for the copper atoms (1.57) of all complexes considered here.

In general, the DFT calculations suggest that for complexes with the same bridging ligand, the dianionic **NBDA** and DPFN complexes exhibit similar bond orders between copper and bridging ligand and a similar charge on the bridging ligand, despite the different (formal) coordination number of copper. The major differences correspond to weaker intermetallic interactions and more ionic character for Cu(I) in the **NBDA** complexes. It is noteworthy that despite the structural resemblance of the bpnp and **NBDA** ligands, only a single bridging chloride is found in **1**. This suggests that the negative charge of the naphthyridine ligand disfavours the accumulation of charged species at the bridging site. This in turn may result in different reactivity of **NBDA**-dicopper complexes compared to those with charge-neutral naphthyridine ligands. As noted previously by Gagnon, complex **1** does not react with oxygen but appears to be oxidized by Ag(I).[46]

The redox properties of the **NBDA** dicopper(I) complexes were analyzed by cyclic voltammetry (CV) in THF solution. The CV of H_2**NBDA** (Figure 5) shows an irreversible reduction around –1.90 V vs. ferrocene, which appears to be composed of two overlapping reduction events that are distinguishable at slow scan rates (Figure SI 11). For the complexes **1** and **3**, a reversible reduction at –2.03 V was observed. A reversible reduction of complex **4** was observed at –1.65 V along with a second reduction with onset at –2.5 V which was not observed for the anionic complexes. Scan rate-dependent measurements of the complexes confirm reversibility of the reduction on the CV timescales (Figures SI 12, SI 13, SI 14). The reversible reduction feature likely involves the **NBDA** ligand and the shift to more positive potentials reflects the reduction in electron density (and negative charge) on the naphthyridine backbone, as calculated for **4**. The irreversible second reduction could not be assigned to a specific process; however, a reduction of the isocyanide ligands at this potential is feasible.[58] Complex **2**, in contrast to the **NBDA** complexes, displays only irreversible redox features (Figure S15): an oxidation at –0.2 V and reductions with onsets at –1.4 V, –2.3 V and –2.7 V.

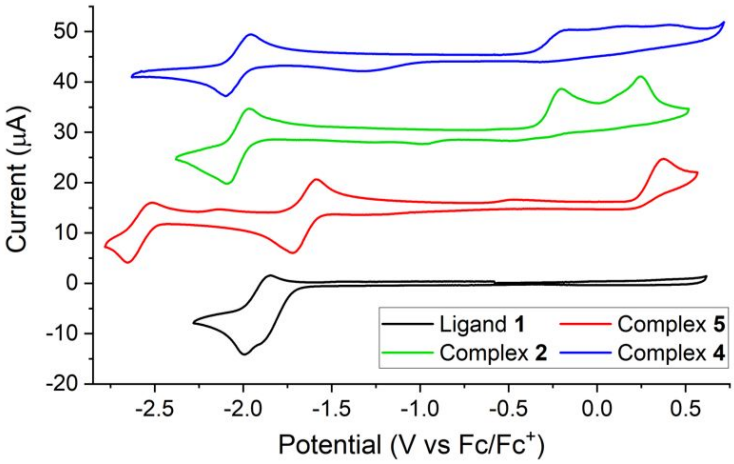

*Figure 5. CVs of H_2**NBDA** and the corresponding dicopper(I) NBDA complexes **2**, **3** and **4**. Conditions: 100 mV/s scan rate; GC working electrode, Pt counter electrode, Ag/$AgBF_4$ reference electrode; 0.1 M Bu_4NPF_6 in THF.*

The oxidations of **1**, **3** and **4** are completely irreversible. Complexes **1** and **3** feature at least two separate oxidation peaks, with the first displaying an onset of -0.35 V and the second occurring around 0 V. A single, irreversible oxidation peak was observed for **4** with an onset at 0.2 V. The oxidation potentials of **1** confirm that Ag(I) is capable of oxidizing the complexes (E^o = 0.41 V vs. ferrocene in THF),[59] consistent with observations previously made by Gagnon and Tolman.[46] The complete lack of reversibility in these dicopper complexes indicates that a rapid change of the molecular structure takes place once an electron is removed. A plausible explanation could be that an oxidation from Cu(I) to Cu(II) initially occurs, but the oxidized copper is susceptible to rapid de-coordination from **NBDA** (due to coordinative unsaturation) under the experimental conditions used here.[60,61] While the naphthyridine bis-amido complexes seem at least somewhat stable to reductive conditions, they appear not to support the transformation of dicopper(I) units to higher oxidation states (at least without additional stabilization by solvent or additional ligands), in contrast to other families of naphthyridine-based ligands.[29,36,37,62]

Conclusions

The straightforward synthesis of the dianionic naphthyridine ligand H_2**NBDA** was achieved through palladium-catalyzed aminocarbonylation. The dicopper(I) complexes with the **NBDA** scaffold were prepared in high yields by reaction of this ligand with CuMes in the presence of either [^{n}Bu_4N]Cl or [^{n}Bu_4N]N_3 to give the corresponding bridging chloride and azide compounds **1** and **3** as overall anionic

complexes. The use of CuMes as a copper source allows rapid metallation of the ligand precursor with elimination of relatively inert mesitylene and avoids deleterious salt-elimination chemistry that might incorporate additional metal ions into the product. In the presence of xylyl isocyanide, an unexpected end-on coordination of two ligands giving an overall neutral dicopper(I) complex was observed.

The solid-state structures of the **NBDA** complexes exhibit large intermetallic separations of 2.98 Å – 3.08 Å between copper(I) sites and trigonal coordination geometries. The large metal-metal distances are induced by the electronic profile of the dianionic ligand: the $Cu–N_{Amide}$ bonds are stronger than the $Cu–N_{Naph}$ bonds (reflected by shorter bonds and higher calculated bond orders). The influence of the increased intermetallic separation induced by the ionic nature of the ligand is most clearly observed with isocyanide. Terminal coordination at each Cu atom is favored over the bridging coordination mode observed with charge-neutral naphthyridine ligands which enforce a shorter Cu–Cu separation of 2.366 Å.[34] The NBDA ligand displays reversible, ligand-based reductions in complexes 1, 3 and 4, although isolation of chemically reduced species was not achieved.

This study suggests that dianionic naphthyridine-based ligands can impart unique properties for bimetallic cores that are expected to compliment those of similar charge-neutral ligands. The modular synthesis of the ligand should also enable straight-forward modification of the substituent of the amide groups, which in turn can be used to tune redox potentials and electron density of the bimetallic complexes. Further studies will explore applications of this class of ligands in bimetallic chemistry and to uncover the effects of a charged ligand scaffold on reactivity.

Conflicts of Interest

There are no conflicts of interest to declare.

Acknowledgements

This work was funded by U.S. Department of Energy, Office of Science, Office of Basic Energy Sciences, Chemical Sciences, Geosciences, and Biosciences Division, under Contract No. DE-AC02-05CH11231. This research used resources of the Advanced Light Source, which is a DOE Office of Science User Facility under contract no. DE-AC02-05CH11231. L.S. gratefully acknowledges the Swiss National Science Foundation for support through an Early Postdoc Mobility grant (Grant number P2ZHP2_191410). The CheXRay facility at UC Berkeley is acknowledged for assistance in acquisition of the crystal structure of **4**. We thank Drs. Hasan Celik, Raynald Giovine, and Pines Magnetic Resonance Center's Core NMR Facility (PMRC Core) for spectroscopic assistance. The instruments used in this work were supported by the PMRC Core. Jose Martinez Fernandez is thanked for helpful feedback and discussions.

References

(1) Peterson, R. L.; Kim, S.; Karlin, K. D. Copper Enzymes. In *Comprehensive Inorganic Chemistry II (Second Edition): From Elements to Applications*; Elsevier, 2013; Vol. 3, pp 149–177. https://doi.org/10.1016/B978-0-08-097774-4.00309-0.

(2) Seefeldt, L. C.; Hoffman, B. M.; Dean, D. R. Mechanism of Mo-Dependent Nitrogenase. *Annu. Rev. Biochem.* **2009**, *78* (1), 701–722. https://doi.org/10.1146/annurev.biochem.78.070907.103812.

(3) Tavares, P.; Pereira, A. S.; Moura, J. J. G.; Moura, I. Metalloenzymes of the Denitrification Pathway. *J. Inorg. Biochem.* **2006**, *100* (12), 2087–2100. https://doi.org/10.1016/j.jinorgbio.2006.09.003.

(4) Gordon, C. P.; Engler, H.; Tragl, A. S.; Plodinec, M.; Lunkenbein, T.; Berkessel, A.; Teles, J. H.; Parvulescu, A. N.; Copéret, C. Efficient Epoxidation over Dinuclear Sites in Titanium Silicalite-1. *Nature* **2020**, *586* (7831), 708–713. https://doi.org/10.1038/s41586-020-2826-3.
(5) Groothaert, M. H.; Smeets, P. J.; Sels, B. F.; Jacobs, P. A.; Schoonheydt, R. A. Selective Oxidation of Methane by the Bis(μ-Oxo)Dicopper Core Stabilized on ZSM-5 and Mordenite Zeolites. *J. Am. Chem. Soc.* **2005**, *127* (5), 1394–1395. https://doi.org/10.1021/ja047158u.
(6) Mankad, N. P. Selectivity Effects in Bimetallic Catalysis. *Chem. - Eur. J.* **2016**, *22* (17), 5822–5829. https://doi.org/10.1002/chem.201505002.
(7) Graziano, B. J.; Scott, T. R.; Vollmer, M. V.; Dorantes, M. J.; Young, V. G.; Bill, E.; Gagliardi, L.; Lu, C. C. One-Electron Bonds in Copper-Aluminum and Copper-Gallium Complexes. *Chem. Sci.* **2022**, *13* (22), 6525–6531. https://doi.org/10.1039/d2sc01998a.
(8) Gavrilova, A. L.; Bosnich, B. Principles of Mononucleating and Binucleating Ligand Design. *Chem. Rev.* **2004**, *104* (2), 349–384. https://doi.org/10.1021/cr020604g.
(9) Dalle, K. E.; Meyer, F. Modelling Binuclear Metallobiosites: Insights from Pyrazole-Supported Biomimetic and Bioinspired Complexes. *Eur. J. Inorg. Chem.* **2015**, *2015* (21), 3391–3405. https://doi.org/10.1002/ejic.201500185.
(10) Prim, D.; Andrioletti, B.; Rose-Munch, F.; Rose, E.; Couty, F. Bimetallic Pd/Cr and Pd/Mn Activation of Carbon-Halide Bonds in Organochromium and Organomanganese Complexes. *Tetrahedron* **2004**, *60* (15), 3325–3347. https://doi.org/10.1016/j.tet.2004.02.002.
(11) Campos, J. Bimetallic Cooperation across the Periodic Table. *Nat. Rev. Chem.* **2020**, *4* (12), 696–702. https://doi.org/10.1038/s41570-020-00226-5.
(12) Krogman, J. P.; Thomas, C. M. Metal–Metal Multiple Bonding in C3-Symmetric Bimetallic Complexes of the First Row Transition Metals. *Chem. Commun.* **2014**, *50* (40), 5115–5127. https://doi.org/10.1039/c3cc47537a.
(13) Zhang, S.; Wang, Q.; Thierer, L. M.; Weberg, A. B.; Gau, M. R.; Carroll, P. J.; Tomson, N. C. Tuning Metal-Metal Interactions through Reversible Ligand Folding in a Series of Dinuclear Iron Complexes. *Inorg. Chem.* **2019**, *58* (18), 12234–12244. https://doi.org/10.1021/acs.inorgchem.9b01673.
(14) Van Den Beuken, E. K.; Feringa, B. L. Bimetallic Catalysis by Late Transition Metal Complexes. *Tetrahedron* **1998**, *54* (43), 12985–13011. https://doi.org/10.1016/S0040-4020(98)00319-6.
(15) Steel, P. J. Ligand Design in Multimetallic Architectures: Six Lessons Learned. *Acc. Chem. Res.* **2005**, *38* (4), 243–250. https://doi.org/10.1021/ar040166v.
(16) Emerson, K.; Emad, A.; Brookes, R. W.; Martin, R. L. Two Magnetically Subnormal Copper Halide Complexes with 1,8-Naphthyridine. *Inorg. Chem.* **1973**, *12* (5), 978–981. https://doi.org/10.1021/ic50123a002.
(17) Gatteschi, D.; Mealli, C.; Sacconi, L. Synthesis and Characterization of the Mixed-Valence Copper Complex Trichlorobis(4-Methyl-1,8-Naphthyridine)Dicopper. *Inorg. Chem.* **1976**, *15* (11), 2774–2778. https://doi.org/10.1021/ic50165a041.
(18) Mealli, C.; Zanobini, F. X-Ray Crystal Structure of the Antiferromagnetic Binuclear Dichloro-μ-Dichloro-μ-Di(1,8-Naphthyridine)-Dicopper Complex. *J. Chem. Soc. Chem. Commun.* **1982**, No. 2, 97–98. https://doi.org/10.1039/C39820000097.
(19) Collin, J. P.; Jouaiti, A.; Sauvage, J. P.; Kaska, W. C.; McLoughlin, M. A.; Keder, N. L.; Harrison, W. T. A.; Stucky, G. D. Synthesis and Electrochemical Characterization of Binuclear Rhodium and Ruthenium Complexes with 1,8-Naphthyridine-2,7-Dicarboxylate. X-Ray Molecular Structure of Tris(μ-Acetato)(1,8-Naphthyridine-2,7-Dicarboxylato)Diruthenium. *Inorg. Chem.* **1990**, *29* (12), 2238–2241. https://doi.org/10.1021/ic00337a012.
(20) He, C.; Lippard, S. J. Design and Synthesis of Multidentate Dinucleating Ligands Based on 1,8-Naphthyridine. *Tetrahedron* **2000**, *56* (42), 8245–8252. https://doi.org/10.1016/S0040-4020(00)00748-1.

(21) Nicolay, A.; Tilley, T. D. Selective Synthesis of a Series of Isostructural MIICuI Heterobimetallic Complexes Spontaneously Assembled by an Unsymmetrical Naphthyridine-Based Ligand. *Chem. - Eur. J.* **2018**, *24* (41), 10329–10333. https://doi.org/10.1002/chem.201802623.
(22) Desnoyer, A. N.; Nicolay, A.; Rios, P.; Ziegler, M. S.; Tilley, T. D. Bimetallics in a Nutshell: Complexes Supported by Chelating Naphthyridine-Based Ligands. *Acc. Chem. Res.* **2020**, *53* (9), 1944–1956. https://doi.org/10.1021/acs.accounts.0c00382.
(23) Bera, J. K.; Sadhukhan, N.; Majumdar, M. 1,8-Naphthyridine Revisited: Applications in Dimetal Chemistry. *Eur. J. Inorg. Chem.* **2009**, *2009* (27), 4023–4038. https://doi.org/10.1002/ejic.200900312.
(24) Zhou, Y. Y.; Hartline, D. R.; Steiman, T. J.; Fanwick, P. E.; Uyeda, C. Dinuclear Nickel Complexes in Five States of Oxidation Using a Redox-Active Ligand. *Inorg. Chem.* **2014**, *53* (21), 11770–11777. https://doi.org/10.1021/ic5020785.
(25) Davenport, T. C.; Ahn, H. S.; Ziegler, M. S.; Tilley, T. D. A Molecular Structural Analog of Proposed Dinuclear Active Sites in Cobalt-Based Water Oxidation Catalysts. *Chem. Commun.* **2014**, *50* (48). https://doi.org/10.1039/c3cc46865h.
(26) Shiota, Y.; Juhász, G.; Yoshizawa, K. Role of Tyrosine Residue in Methane Activation at the Dicopper Site of Particulate Methane Monooxygenase: A Density Functional Theory Study. *Inorg. Chem.* **2013**, *52* (14), 7907–7917. https://doi.org/10.1021/ic400417d.
(27) Bienenmann, R. L. M.; Loyo, A. O.; Lutz, M.; Broere, D. L. J. Mechanistic Investigation into Copper(I) Hydride Catalyzed Formic Acid Dehydrogenation. *ACS Catal.* **2024**, 15599–15608. https://doi.org/10.1021/acscatal.4c05008.
(28) Tikkanen, W. R.; Carl, K.; Bomben, K. D.; Jolly, W. L.; Kaska, W. C.; Ford, P. C. Synthesis, Characterization, and x-Ray Molecular Structures of Mono-and Dinuclear Copper Complexes with 2, 7-Bis(2-Pyridyl)-1, 8-Naphthyridine. *Inorg. Chem.* **1984**, *23* (22), 3633–3638. https://doi.org/10.1021/ic00190a041.
(29) Kounalis, E.; Lutz, M.; Broere, D. L. J. Cooperative H2 Activation on Dicopper(I) Facilitated by Reversible Dearomatization of an "Expanded PNNP Pincer" Ligand. *Chem. - Eur. J.* **2019**, *25* (58), 13280–13284. https://doi.org/10.1002/chem.201903724.
(30) Scheerder, A. R.; Lutz, M.; Broere, D. L. J. Unexpected Reactivity of a PONNOP "expanded Pincer" Ligand. *Chem. Commun.* **2020**, *56* (59), 8198–8201. https://doi.org/10.1039/d0cc02166k.
(31) Hall, P. D.; Stevens, M. A.; Wang, J. Y. J.; Pham, L. N.; Coote, M. L.; Colebatch, A. L. Copper and Zinc Complexes of 2,7-Bis(6-Methyl-2-Pyridyl)-1,8-Naphthyridine A Redox-Active, Dinucleating Bis(Bipyridine) Ligand. *Inorg. Chem.* **2022**, *61* (48), 19333–19343. https://doi.org/10.1021/acs.inorgchem.2c03126.
(32) Delaney, A. R.; Yu, L.-J.; Coote, M. L.; Colebatch, A. L. Synthesis of an Expanded Pincer Ligand and Its Bimetallic Coinage Metal Complexes. *Dalton Trans.* **2021**, *50* (34), 11909–11917. https://doi.org/10.1039/D1DT01741A.
(33) Boehm, E. D.; Fronczek, F. R.; Fox, S. Dibromo and Diiodo-Bridged Dicopper(I,I) Complexes of 1,8-Naphthyridine-2,7-Di(N-Cyclohexyl)Methanimine. *J. Chem. Crystallogr.* **2022**, *52* (4), 485–493. https://doi.org/10.1007/s10870-022-00920-w.
(34) Davenport, T. C.; Tilley, T. D. Dinucleating Naphthyridine-Based Ligand for Assembly of Bridged Dicopper(i) Centers: Three-Center Two-Electron Bonding Involving an Acetonitrile Donor. *Angew. Chem. - Int. Ed.* **2011**, *50* (51), 12205–12208. https://doi.org/10.1002/anie.201106081.
(35) Ziegler, M. S.; Levine, D. S.; Lakshmi, K. V.; Tilley, T. D. Aryl Group Transfer from Tetraarylborato Anions to an Electrophilic Dicopper(I) Center and Mixed-Valence μ-Aryl Dicopper(I,II) Complexes. *J. Am. Chem. Soc.* **2016**, *138* (20), 6484–6491. https://doi.org/10.1021/jacs.6b00802.
(36) Ziegler, M. S.; Torquato, N. A.; Levine, D. S.; Nicolay, A.; Celik, H.; Tilley, T. D. Dicopper Alkyl Complexes: Synthesis, Structure, and Unexpected Persistence. *Organometallics* **2018**, *37* (16), 2807–2823. https://doi.org/10.1021/acs.organomet.8b00443.

(37) Desnoyer, A. N.; Nicolay, A.; Ziegler, M. S.; Lakshmi, K. V.; Cundari, T. R.; Tilley, T. D. A Dicopper Nitrenoid by Oxidation of a CuICuICore: Synthesis, Electronic Structure, and Reactivity. *J. Am. Chem. Soc.* **2021**, *143* (18), 7135–7143. https://doi.org/10.1021/jacs.1c02235.
(38) Ríos, P.; See, M. S.; Handford, R. C.; Cooper, J. K.; Tilley, T. D. Tetracopper σ-Bound μ-Acetylide and -Diyne Units Stabilized by a Naphthyridine-Based Dinucleating Ligand. *Angew. Chem. Int. Ed.* **2023**, *62* (45), e202310307. https://doi.org/10.1002/anie.202310307.
(39) Ríos, P.; See, M. S.; Handford, R. C.; Teat, S. J.; Tilley, T. D. Robust Dicopper(I) μ-Boryl Complexes Supported by a Dinucleating Naphthyridine-Based Ligand. *Chem. Sci.* **2022**, *13* (22), 6619–6625. https://doi.org/10.1039/D2SC00848C.
(40) Dudev, T.; Lim, C. Competition among Metal Ions for Protein Binding Sites: Determinants of Metal Ion Selectivity in Proteins. *Chem. Rev.* **2014**, *114* (1), 538–556. https://pubs.acs.org/doi/10.1021/cr4004665.
(41) Solomon, E. I.; Heppner, D. E.; Johnston, E. M.; Ginsbach, J. W.; Cirera, J.; Qayyum, M.; Kieber-Emmons, M. T.; Kjaergaard, C. H.; Hadt, R. G.; Tian, L. Copper Active Sites in Biology. *Chem. Rev.* **2014**, *114* (7), 3659–3853. https://doi.org/10.1021/cr400327t.
(42) Mandal, M.; Elwell, C. E.; Bouchey, C. J.; Zerk, T. J.; Tolman, W. B.; Cramer, C. J. Mechanisms for Hydrogen-Atom Abstraction by Mononuclear Copper(III) Cores: Hydrogen-Atom Transfer or Concerted Proton-Coupled Electron Transfer? *J. Am. Chem. Soc.* **2019**, *141* (43), 17236–17244. https://doi.org/10.1021/jacs.9b08109.
(43) Dhar, D.; Tolman, W. B. Hydrogen Atom Abstraction from Hydrocarbons by a Copper(III)-Hydroxide Complex. *J. Am. Chem. Soc.* **2015**, *137* (3), 1322–1329. https://doi.org/10.1021/ja512014z.
(44) Donoghue, P. J.; Tehranchi, J.; Cramer, C. J.; Sarangi, R.; Solomon, E. I.; Tolman, W. B. Rapid C-H Bond Activation by a Monocopper(III)-Hydroxide Complex. *J. Am. Chem. Soc.* **2011**, *133* (44), 17602–17605. https://doi.org/10.1021/ja207882h.
(45) Lee, C. H.; Wu, C. L.; Hua, S. A.; Liu, Y. H.; Peng, S. M.; Liu, S. T. Complexation of Tetrakis(Acetato)Chloridodiruthenium with Naphthyridine-2,7-Dicarboxylate - Characterization and Catalytic Activity. *Eur. J. Inorg. Chem.* **2015**, *2015* (8), 1417–1423. https://doi.org/10.1002/ejic.201403156.
(46) Gagnon, N. Synthetic And Spectroscopic Investigation Of Mono And Dinuclear Copper-Oxygen Complexes, University of Minnesota Twin Cities, 2018. http://conservancy.umn.edu/handle/11299/215163.
(47) El-ghayoury, A.; Ziessel, R. A Convenient Synthetic Route to Polypyridine-Esters by Palladium-Promoted Carboalkoxylation. *Tetrahedron Lett.* **1998**, *39* (25), 4473–4476. https://doi.org/10.1016/S0040-4039(98)00820-X.
(48) Hung, M. U.; Liao, B. S.; Liu, Y. H.; Peng, S. M.; Liu, S. T. Dicopper Complexes Catalyzed Coupling/Cyclization of 2-Bromobenzoic Acids with Amidines Leading to Quinazolinones. *Appl. Organomet. Chem.* **2014**, *28* (9), 661–665. https://doi.org/10.1002/aoc.3177.
(49) Zhang, Y.; Tong, P.; Yang, D.; Li, J.; Wang, B.; Qu, J. Migratory Insertion and Hydrogenation of a Bridging Azide in a Thiolate-Bridged Dicobalt Reaction Platform. *Chem. Commun.* **2017**, *53* (71), 9854–9857. https://doi.org/10.1039/C7CC05092E.
(50) Tran, B. L.; Krzystek, J.; Ozarowski, A.; Chen, C.; Pink, M.; Karty, J. A.; Telser, J.; Meyer, K.; Mindiola, D. J. Formation and Reactivity of the Terminal Vanadium Nitride Functionality. *Eur. J. Inorg. Chem.* **2013**, *2013* (22–23), 3916–3929. https://doi.org/10.1002/ejic.201300178.
(51) Grant, L. N.; Pinter, B.; Gu, J.; Mindiola, D. J. Molecular Zirconium Nitride Super Base from a Mononuclear Parent Imide. *J. Am. Chem. Soc.* **2018**, *140* (50), 17399–17403. https://doi.org/10.1021/jacs.8b11198.
(52) Dori, Z.; Ziolo, R. F. The Chemistry of Coordinated Azides. *Chem. Rev.* **1973**, *73* (3), 247–254. https://doi.org/10.1021/cr60283a003.
(53) Salehi, S. M.; Koner, D.; Meuwly, M. Vibrational Spectroscopy of N3– in the Gas and Condensed Phase. *J. Phys. Chem. B* **2019**, *123* (15), 3282–3290. https://doi.org/10.1021/acs.jpcb.8b11430.

(54) Hart, M. D.; Meyers, J. J.; Wood, Z. A.; Nakakita, T.; Applegate, J. C.; Erickson, N. R.; Gerasimchuk, N. N.; Barybin, M. V. Tuning π-Acceptor/σ-Donor Ratio of the 2-Isocyanoazulene Ligand: Non-Fluorinated Rival of Pentafluorophenyl Isocyanide and Trifluorovinyl Isocyanide Discovered. *Molecules* **2021**, *26* (4), 981. https://doi.org/10.3390/molecules26040981.

(55) Melekhova, A. A.; Novikov, A. S.; Luzyanin, K. V.; Bokach, N. A.; Starova, G. L.; Gurzhiy, V. V.; Kukushkin, V. Y. Tris-Isocyanide Copper(I) Complexes: Synthetic, Structural, and Theoretical Study. *Inorganica Chim. Acta* **2015**, *434*, 31–36. https://doi.org/10.1016/J.ICA.2015.05.002.

(56) Pruchnik, F. P.; Duraj, S. A. Isocyanide Complexes. In *Organometallic Chemistry of the Transition Elements*; Pruchnik, F. P., Duraj, S. A., Eds.; Springer US: Boston, MA, 1990; pp 617–645. https://doi.org/10.1007/978-1-4899-2076-8_12.

(57) Chai, J.-D.; Head-Gordon, M. Systematic Optimization of Long-Range Corrected Hybrid Density Functionals. *J. Chem. Phys.* **2008**, *128* (8), 084106. https://doi.org/10.1063/1.2834918.

(58) Niznik, G. E.; Walborsky, H. M. Isocyanide Reductions. A Convenient Method for Deamination. *J. Org. Chem.* **1978**, *43* (12), 2396–2399. https://doi.org/10.1021/jo00406a020.

(59) Connelly, N. G.; Geiger, W. E. Chemical Redox Agents for Organometallic Chemistry. *Chem. Rev.* **1996**, *96* (2), 877–910. https://doi.org/10.1021/cr940053x.

(60) Li, D.; Ollevier, T. Mechanism Studies of Oxidation and Hydrolysis of Cu(I)–NHC and Ag–NHC in Solution under Air. *J. Organomet. Chem.* **2020**, *906*, 121025. https://doi.org/10.1016/j.jorganchem.2019.121025.

(61) Herrmann, H.; Kaifer, E.; Himmel, H. J. Hydrogen-Atom Transfer (HAT) Initiated by Intramolecular Ligand–Metal Electron Transfer. *Chem. - Eur. J.* **2017**, *23* (23), 5520–5528. https://doi.org/10.1002/chem.201605971.

(62) He, C.; Lippard, S. J. Synthesis and Characterization of Several Dicopper(I) Complexes and a Spin-Delocalized Dicopper(I,II) Mixed-Valence Complex Using a 1,8-Naphthyridine-Based Dinucleating Ligand. *Inorg. Chem.* **2000**, *39* (23), 5225–5231. https://doi.org/10.1021/ic0005339.

Data Availability Statement

The data supporting this article have been included as part of the Supplementary Information. Additionally, the crystallographic data for complexes **1**, **2**, **3** and **4** have been deposited at CCDC with the following accession numbers: 2414945 (**1**), 2414942 (**2**), 2414944 (**3**), 2414943 (**4**).